Thermalization and Cooling of Plasmon-Exciton Polaritons: Towards Quantum Condensation

S. R. K. Rodriguez,[1,*] J. Feist,[2,†] M. A. Verschuuren,[3] F. J. Garcia Vidal,[2] and J. Gómez Rivas[1,4]

[1]*Center for Nanophotonics, FOM Institute AMOLF, c/o Philips Research Laboratories, High Tech Campus 4, 5656 AE Eindhoven, The Netherlands*

[2]*Departamento de Física Teórica de la Materia Condensada and Condensed Matter Physics Center (IFIMAC), Universidad Autónoma de Madrid, 28049 Madrid, Spain*

[3]*Philips Research Laboratories, High Tech Campus 4, 5656 AE Eindhoven, The Netherlands*

[4]*COBRA Research Institute, Eindhoven University of Technology, P.O. Box 513, 5600 MB Eindhoven, The Netherlands*

(Received 6 June 2013; revised manuscript received 2 August 2013; published 18 October 2013)

We present indications of thermalization and cooling of quasiparticles, a precursor for quantum condensation, in a plasmonic nanoparticle array. We investigate a periodic array of metallic nanorods covered by a polymer layer doped with an organic dye at room temperature. Surface lattice resonances of the array—hybridized plasmonic-photonic modes—couple strongly to excitons in the dye, and bosonic quasiparticles which we call plasmon-exciton polaritons (PEPs) are formed. By increasing the PEP density through optical pumping, we observe thermalization and cooling of the strongly coupled PEP band in the light emission dispersion diagram. For increased pumping, we observe saturation of the strong coupling and emission in a new weakly coupled band, which again shows signatures of thermalization and cooling.

DOI: 10.1103/PhysRevLett.111.166802 PACS numbers: 73.20.Mf, 33.57.+c, 42.50.−p, 71.36.+c

Surface plasmon polaritons (SPPs) are light-matter quasiparticles at a metal-dielectric interface, enabling control of light on subwavelength scales [1]. SPPs are bosons, and by virtue of bosonic stimulation, transition rates into a quantum state are enhanced when the final state occupation exceeds unity. Bosonic stimulation underlies the laser through stimulated emission, and condensation through stimulated scattering. The former has allowed plasmonics to open a new era of nanoscopic coherent light sources [2–5]. In contrast, condensation of SPPs into a single quantum state appears to have never been considered. The reasons for this are likely manifold. Propagating SPPs do not have a cutoff—their ground state is at zero frequency, such that thermalization is not number-conserving and condensation does not occur. On the other hand, localized surface plasmon resonances (LSPRs) have a flat dispersion, implying infinite effective mass. Condensation is more easily achieved with low-mass quasiparticles, as it occurs when the mean thermal wavelength $\lambda_T \propto (mk_BT)^{-1/2}$ exceeds the interparticle spacing. Additionally, the quasiparticles have to thermalize, which poses a challenge for plasmonic systems with typical lifetimes $\lesssim 10$ fs.

One system that may overcome the aforementioned limitations is a periodic array of metallic nanoparticles covered by organic molecules in solid state. LSPRs in the nanoparticles hybridize with diffraction orders radiating in the plane of the array (so-called Rayleigh anomalies), leading to surface lattice resonances (SLRs) [6–11]. While the SPP-exciton strong coupling has been investigated for propagating modes in flat [12–14] and perforated [15–17] metallic layers, as well as for localized modes in nanostructures [18–20], the strong coupling of SLRs to excitons remains unexplored. Advantageously, SLRs can have a narrow linewidth (few meVs [6]) and tunable dispersion via the nanoparticle geometry and lattice constant [21,22], thereby supporting low-mass polaritons with relatively long lifetimes. As shown below, strongly coupled SLR-exciton quasiparticles are low-mass ($\sim 10^{-7}$ times the electron rest mass) analogues of exciton polaritons in semiconductor microcavities, for which condensation has been observed in several groundbreaking experiments [23–25]. We therefore call them plasmon-exciton polaritons (PEPs).

In this Letter, we demonstrate the suitability of PEPs in metallic nanoparticle arrays for quantum condensation. We show that they thermalize, with their effective temperature approaching the lattice temperature when their density is increased through optical pumping. In the present system, we observe a saturation of the strong SLR-exciton coupling before condensation sets in. This leads to a transition from strong to weak coupling, after which we observe thermalization and cooling of the weakly coupled SLR mode.

Figure 1 illustrates the sample. A periodic array of silver nanorods was fabricated onto a fused silica substrate by substrate conformal nanoimprint lithography [26]. A scanning electron microscope image of the resist layer used for the fabrication is shown in Fig. 1(b). The rod dimensions are $230 \times 70 \times 20\ \mathrm{nm}^3$, with lattice constants $a_x = 380$ nm and $a_y = 200$ nm. A 20 nm layer of Si_3N_4 on top of the array prevents the silver from oxidizing. A 300 nm layer of polyvinyl alcohol (PVA)—with rhodamine 6G (R6G) dye molecules for the emission experiments—was spin coated on top. Figure 1(c) shows the absorptance and the normalized emission of the R6G layer. All experiments were

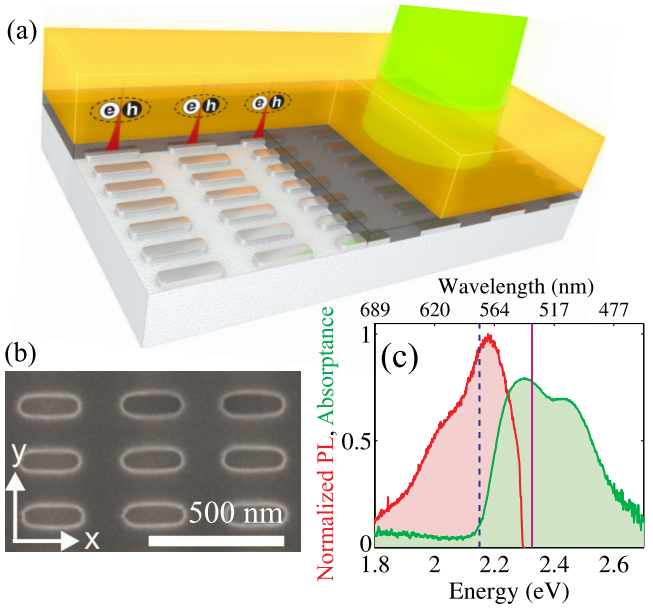

FIG. 1 (color online). (a) A silver nanorod array on a SiO_2 substrate covered by a thin Si_3N_4 layer (gray) and a R6G-PVA layer (orange). An incident laser (green) pumps the R6G exciton reservoir. (b) Scanning electron microscope image of the resist layer used for the fabrication of the nanorod array. (c) Normalized photoluminescence (PL) (red) and absorptance (green) of the R6G layer without the nanorod array. The solid line indicates the pump energy, while the dashed line indicates the emission energy of the saturated ground state at the highest pump power.

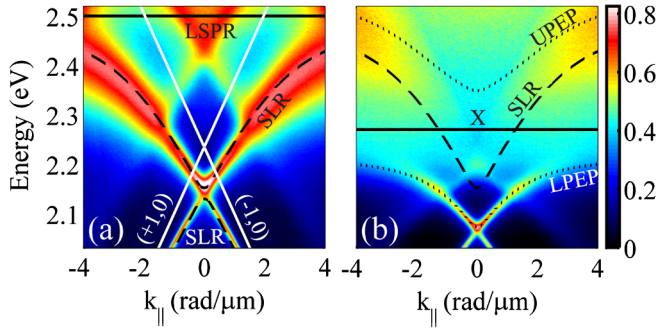

FIG. 2 (color online). Extinction spectra of the nanorod array covered by a polymer layer (a) without and (b) with R6G molecules, both in the same color scale. In (a) the solid white lines indicate the Rayleigh anomalies, while the solid black line indicates the localized surface plasmon resonance. The dashed lines indicate the surface lattice resonances. In (b) the solid line indicates the R6G exciton, the dashed line is the upper SLR from (a), and the dotted lines indicate the mixed states (plasmon-exciton polaritons).

performed at room temperature (300 K). Further details are included in the Supplemental Material [27].

We first analyze the strongly coupled modes in the nanorod array. Figure 2 shows two light extinction measurements: In Fig. 2(a) the PVA layer has no R6G molecules, while in Fig. 2(b) R6G molecules were embedded at 23 wt % with respect to the PVA (R6G number density $\approx 3.6 \times 10^8$ μm^{-3}). The extinction, defined as $1 - T_0$ with T_0 the zeroth-order transmittance, is shown in color as a function of the incident photon energy and wave vector component $k_\parallel$ parallel to the long axis of the nanorods (x axis). The incident light is s-polarized, probing the short axis of the nanorods (y axis).

The dispersive extinction peaks in Fig. 2(a) are SLRs associated with the (± 1, 0) diffraction orders. These hybrid modes arise from the coupling between the LSPR (solid black line) and the (± 1, 0) Rayleigh anomalies (intersecting solid white lines). The SLRs (dashed black lines) are calculated with a 3×3 model Hamiltonian including the decay of the three modes and their mutual coupling (see Supplemental Material for details [27]). A small gap between the upper and lower SLRs is observed at normal incidence near 2.15 eV, where only the upper SLR is excited due to the mode symmetries. The electric field distribution in the plane of the array is symmetric for the upper SLR, but antisymmetric for the lower SLR, which renders the former "bright" and the latter "dark" [22].

Figure 2(b) shows the extinction of the same array but with the R6G molecules embedded in the PVA. The solid line indicates the peak energy of the R6G exciton. The dashed line is the upper SLR as shown in Fig. 2(a). PEPs are composite quasiparticles emerging from the strong coupling of these two resonances, which we model with a 2×2 Hamiltonian [27]. The inhomogeneity in the coupling between molecules and SLRs enters into the properties of the collective Dicke state that forms the excitonic part of the 2×2 Hamiltonian, but does not further influence the dynamics [14,28]. We ignore the LSPR and lower SLR because they have minimal influence in what follows. The upper and lower PEPs, indicated by the dotted lines in Fig. 2(b), display a 250 meV Rabi splitting at zero SLR-exciton detuning. The extinction of the upper PEP band is smeared out due to the increased SLR linewidth at higher energies, and possibly due to the influence of another mode [see near 2.4 eV at $k_\parallel = 0$ in Fig. 2(a)]. However, this has minimal influence on the lower PEP. Analogous to the Hopfield coefficients [29], the exciton coefficient $x(k_\parallel)$ and SLR coefficient $s(k_\parallel)$ characterize the relative contributions to the PEP. We find $|x(0)|^2 = 0.3$ and $|s(0)|^2 = 0.7$ for the lower PEP at $k_\parallel = 0$. Thus, despite the large SLR-exciton detuning (-118 meV), the exciton fraction is not negligible. Near $k_\parallel = 0$, the effective mass of the lower PEP is $m_p^* \approx \hbar^2/(\partial^2 E/\partial k_\parallel^2) \approx 2.0 \times 10^{-37}$ kg. These PEPs are 10^{10}–10^{12} times lighter than atoms [30,31], and $\sim$100 times lighter than exciton polaritons [32]. The characteristic temperatures ($\sim$1000 K) in our system are correspondingly higher (keeping the mass-to-temperature ratio similar): about 10^8–10^{11} times higher than in atomic Bose-Einstein condensation systems [30,31], and $\sim 10^2$ times higher than GaAs and CdTe exciton-polariton

systems [32]. Note that recent GaN and ZnO exciton-polariton systems can operate at room temperature [33].

In Fig. 3 we present a series of emission measurements obtained by increasingly pumping the structure in Fig. 2(b) with an optical parametric oscillator having peak energy 2.33 eV, ~200 fs pulses, and 80 MHz repetition rate. The sample is fixed, while the detector rotates collecting s polarized light with in-plane momentum $k_{\|}$ along $\hat{x}$ [27]. Figure 3(a) shows the forward ($k_{\|} = 0$) emission spectrum as a function of the pump irradiance. The peak at ~2.08 eV, which dominates the spectrum below a critical irradiance of $P_c \approx 60\ \mathrm{W/cm^2}$, is the emission from the lower PEP. The shoulder at 2.065 eV is attributed to the lower SLR, which is dark at $k_{\|} = 0$ but appears in the spectrum due to the finite angular resolution of the experiment. As pumping increases, the lower PEP peak blueshifts and broadens. Above P_c a new peak emerges at ~2.15 eV, and at $\sim 2P_c$ its emission exceeds the lower PEP emission. We attribute the shift of the coupled states towards the uncoupled states to saturation of the coupling with increasing exciton density [34,35]. This has previously been observed in plasmon-exciton polariton systems as a diminished normal mode splitting in the frequency domain, and as a reduced Rabi frequency in the time domain [36,37].

Instead of a smooth transition of the peak energy, we observe the coexistence of two bands at intermediate pump powers. This is explained by a model taking into account the spatiotemporal profile of the excitation density. We assume that the exciton-SLR coupling saturates as $\Omega_{\mathrm{XS}} = \Omega_{\mathrm{XS},0}[1 + n(r,t)/n_{\mathrm{sat}}]^{-1/2}$, with the excitation density n varying spatially over the pump beam profile and decaying in time after the pump. The emission from each point in space and time is then assumed to be at the PEP energy given by inserting this Ω_{XS} into the two-state model used for modeling the PEP. At zero detuning, strong coupling occurs when the energy exchange rate Ω_{XS} is larger than the decay rates γ_X and γ_S of the exciton and SLR, respectively. Although the distinction becomes somewhat ambiguous for nonzero detuning as in the present case, the two extreme cases can be readily identified: Small n leads to strong coupling ($\Omega_{\mathrm{XS}} \gg \gamma_X, \gamma_S$), while $n \gg n_{\mathrm{sat}}$ gives weak coupling ($\Omega_{\mathrm{XS}} \ll \gamma_X, \gamma_S$). Integrating over space and time gives the model spectra shown in Fig. 3(b) [27], which agree well with the experimental data. From the model, it follows that the low-energy peak stems from regions with low n where the emission from the strongly coupled PEPs dominates, while the high-energy peak stems from regions with high n where the emission from the weakly coupled SLR dominates. The intermediate regions form a broad background that is not resolved as an isolated peak. Accordingly, for increased pumping the lower PEP emission saturates, while the new band blueshifts towards the bare SLR state and grows in intensity. The experimental output versus input power dependence confirms this [27].

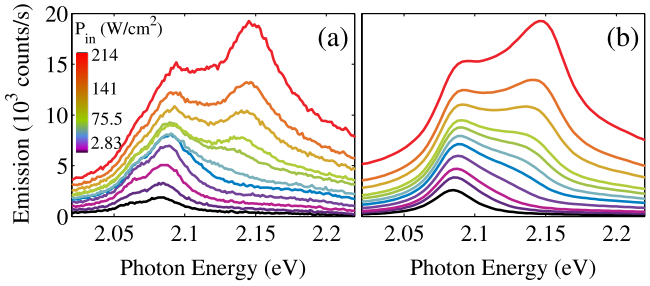

FIG. 3 (color online). Emission at $k_{\|} = 0$, (a) for different experimental input power densities encoded in color, and (b) predicted by a model based on local saturation of the coupling (see text for details).

We now study the dispersion of the observed bands through their angle-dependent emission intensity, shown in Figures 4(a)–4(h) for several pump powers. We find that the lower PEP band is slightly blueshifted compared to the extinction measurements. It is also flatter, corresponding to a slightly higher effective mass of $\approx 2.6 \times 10^{-37}$ kg (extracted from the curvature of the band at $k_{\|} = 0$). We attribute this to a well-known difference between extinction and emission spectra: Extinction stems from the interference between direct and scattered radiation, while emission does not contain a direct part. This leads to a shift of the peak emission energy [38], which can also affect the extracted effective mass if it is angle-dependent. For high pumping, the peak of the emission is slightly redshifted from the SLR peak in extinction. According to our model, this implies that the coupling is not fully saturated—the underlying SLR energy used for the model in Fig. 3(b) is again slightly blueshifted compared to extinction [27].

Next, we discuss the thermalization behavior. Condensation as a thermodynamic phase transition requires the system to approach thermal equilibrium, which constrains the ratio of thermalization to decay time. For inorganic exciton polaritons, both of these times are 1–10 ps, and consequently both equilibrium and nonequilibrium condensation have been observed [32]. For the present system, we estimate a PEP lifetime of at least ~17 fs from the emission linewidth. Vibrational relaxation of R6G, and thus PEP-phonon scattering, occurs on a scale of ~100 fs [39], while PEP-PEP scattering rates are currently unknown. Therefore, equilibrium dynamics seem unlikely in our case. As we show next, we nevertheless observe thermalization and cooling for increased pumping, possibly due to more efficient PEP-PEP scattering at high density.

Figures 4(a)–4(d) display a greater emission from the strongly coupled band at low pumping, while Figs. 4(e)–4(h) display a greater emission from the weakly coupled band at high pumping. We study this in detail by analyzing the occupation n_{oc} as a function of the emitted photon energy, shown in Fig. 4(i) for the strongly coupled band and in Fig. 4(j) for the weakly coupled band. The occupation is

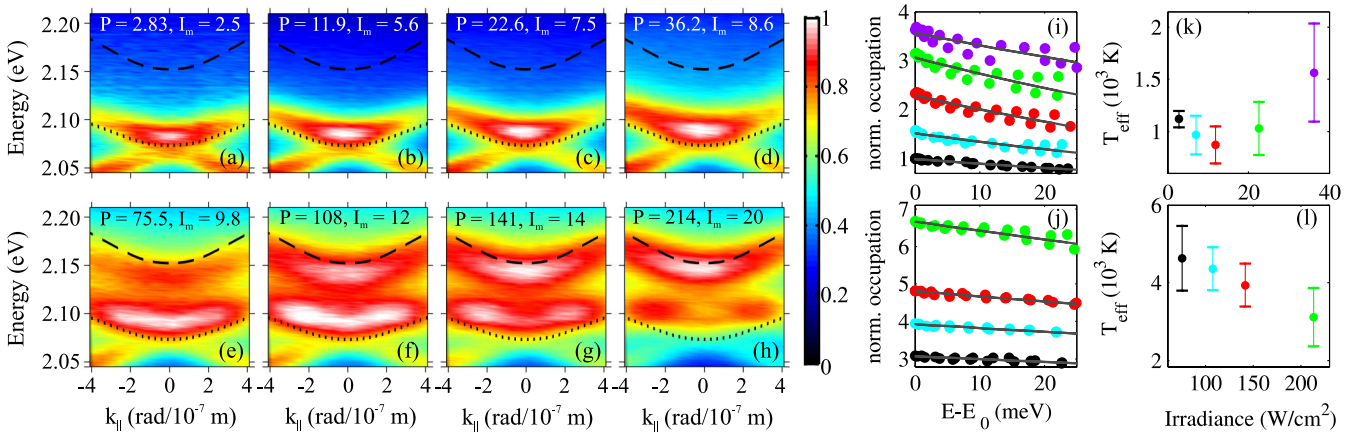

FIG. 4 (color online). (a)–(h) Emission for increasing pump irradiance P (labeled in W/cm^2). The color bar pertains to all spectra, with the maximum intensity I_m indicated in 10^3 counts/s. The dashed and dotted lines are the SLR and PEP energies as in Fig. 2(b). The scale is different from Fig. 2 to magnify the emission near $k_\parallel = 0$. (i),(j) Normalized occupation of the (i) lower (PEP) band below criticality and (j) upper (SLR) band above criticality. Data points of different colors correspond to different P. The two groups of points for each P correspond to the occupation for $\pm k_\parallel$; i.e., the data are slightly asymmetric. The solid gray lines are Maxwell-Boltzmann fits. The mapping between P and color can be inferred from (k) and (l), which show effective temperatures retrieved from the fits in (i) and (j), respectively.

extracted from the emission intensity $I(k_\parallel)$ along the corresponding band, integrated over a fixed bandwidth of 40 meV. We take into account that PEPs are composite quasiparticles and only their photonic component leaks out of the open system. Thus, as in exciton-polariton systems [35,40], we correct for the SLR fraction $|s(k_\parallel)|^2$, giving $n_{oc} \propto I(k_\parallel)/|s(k_\parallel)|^2$. Here we have assumed that SLRs mainly decay radiatively due to their large Rayleigh anomaly fraction and the predominantly radiative decay of LSPRs. The gray lines in Figs. 4(i) and 4(j) are fits of the occupation to a Maxwell-Boltzmann distribution $n_{oc} \propto \exp[-(E - E_0)/k_B T_{\text{eff}}]$, from which we extract the effective temperature T_{eff}. This is shown as a function of the pump irradiance in Figs. 4(k) and 4(l) for the strongly and weakly coupled band, respectively. The error bars represent a 2σ ($\approx 95\%$) confidence interval, and stem mostly from a small asymmetry of n_{oc} for positive and negative $k_\parallel$. This is possibly due to angle-dependent variations in collection efficiency and intensity fluctuations during the measurement time.

The effective temperature of the strongly coupled PEPs displays an initial decrease, but remains warmer than the lattice. This observation, which is reminiscent of early works on exciton-polariton condensates [23,25], indicates that the system approaches but does not fully reach thermal equilibrium with the heat bath (the molecule phonons). In addition, we observe that for increased pumping the ground state ($E - E_0 = 0$) occupation increases slightly above the Maxwell-Boltzmann fit. This could be an indication that the bosonic statistics of the PEPs are becoming relevant, implying that condensation is being approached, although not reached. Consequently, the ground state occupation remains much lower than in exciton-polariton condensates [24,25]. As the power increases and saturation is approached, T_{eff} increases again, although the experimental uncertainty from the fits also increases. This increased uncertainty implies a stronger deviation of the n_{oc} from a thermal distribution near the strong-to-weak coupling transition. Therefore, while cooling of PEPs is observed, saturation of the SLR-exciton coupling sets in before condensation is reached, and the new band with weaker coupling emerges and blueshifts towards the bare SLR state. The effective temperatures in this new band [Fig. 4(l)] are higher than in the PEP band. Nevertheless, T_{eff} decreases monotonically as pumping increases. This cooling implies that condensation of bare SLRs could be within reach, analogous to the condensation of cavity photons observed by Klaers *et al.* [41]. Currently, further pumping was not possible because the molecules bleached. A different pump source or dye could circumvent this limitation, enabling higher excitation densities. We note that SLR lasing has recently been demonstrated by Zhou and co-workers [42].

In conclusion, we presented experimental indications of thermalization and cooling of quasiparticles in an array of Ag nanoparticles covered by organic molecules. This array supports surface lattice resonances, which form plasmon-exciton polaritons through strong coupling to molecular excitons. In view of the low PEP mass, which is furthermore tunable via the surface lattice resonance dispersion, we believe that plasmonics holds great promise for solid-state studies of macroscopic quantum many-body physics at and above room temperature. While the short lifetimes of plasmons make thermodynamic equilibrium challenging, we envisage these results to open a new avenue for studying nonequilibrium quantum dynamics.

We thank Francesca Marchetti for stimulating discussions. This work was supported by the Netherlands Foundation for Fundamental Research on Matter (FOM) and the Netherlands Organization for Scientific Research (NWO), and is part of an industrial partnership program between Philips and FOM. J. F. and F. J. G. V. acknowledge support by the European Research Council under Grant No. 290981 (PLASMONANOQUANTA).

*s.rodriguez@amolf.nl
†johannes.feist@uam.es

[1] W. L. Barnes, A. Dereux, and T. W. Ebbesen, Nature (London) **424**, 824 (2003).
[2] D. J. Bergman and M. I. Stockman, Phys. Rev. Lett. **90**, 027402 (2003).
[3] M. Noginov, G. Zhu, A. M. Belgrave, R. Bakker, V. M. Shalaev, E. E. Narimanov, S. Stout, E. Herz, T. Suteewong, and U. Wiesner, Nature (London) **460**, 1110 (2009).
[4] R. F. Oulton, V. J. Sorger, T. Zentgraf, R.-M. Ma, C. Gladden, L. Dai, G. Bartal, and X. Zhang, Nature (London) **461**, 629 (2009).
[5] O. Hess, J. B. Pendry, S. A. Maier, R. F. Oulton, J. M. Hamm, and K. L. Tsakmakidis, Nat. Mater. **11**, 573 (2012).
[6] S. Zou and G. C. Schatz, J. Chem. Phys. **121**, 12606 (2004).
[7] F. J. García de Abajo, Rev. Mod. Phys. **79**, 1267 (2007).
[8] Y. Chu, E. Schonbrun, T. Yang, and K. B. Crozier, Appl. Phys. Lett. **93**, 181108 (2008).
[9] B. Auguié and W. L. Barnes, Phys. Rev. Lett. **101**, 143902 (2008).
[10] V. G. Kravets, F. Schedin, and A. N. Grigorenko, Phys. Rev. Lett. **101**, 087403 (2008).
[11] G. Vecchi, V. Giannini, and J. G. Rivas, Phys. Rev. Lett. **102**, 146807 (2009).
[12] J. Bellessa, C. Bonnand, J. C. Plenet, and J. Mugnier, Phys. Rev. Lett. **93**, 036404 (2004).
[13] T. K. Hakala, J. J. Toppari, A. Kuzyk, M. Pettersson, H. Tikkanen, H. Kunttu, and P. Törmä, Phys. Rev. Lett. **103**, 053602 (2009).
[14] A. González-Tudela, P. A. Huidobro, L. Martín-Moreno, C. Tejedor, and F. J. García-Vidal, Phys. Rev. Lett. **110**, 126801 (2013).
[15] J. Dintinger, S. Klein, F. Bustos, W. L. Barnes, and T. W. Ebbesen, Phys. Rev. B **71**, 035424 (2005).
[16] P. Vasa, R. Pomraenke, S. Schwieger, Y. I. Mazur, V. Kunets, P. Srinivasan, E. Johnson, J. E. Kihm, D. S. Kim, E. Runge, G. Salamo, and C. Lienau, Phys. Rev. Lett. **101**, 116801 (2008).
[17] T. Schwartz, J. A. Hutchison, C. Genet, and T. W. Ebbesen, Phys. Rev. Lett. **106**, 196405 (2011).
[18] Y. Sugawara, T. A. Kelf, J. J. Baumberg, M. E. Abdelsalam, and P. N. Bartlett, Phys. Rev. Lett. **97**, 266808 (2006).
[19] N. I. Cade, T. Ritman-Meer, and D. Richards, Phys. Rev. B **79**, 241404 (2009).
[20] A. Manjavacas, F. Garcia de Abajo, and P. Nordlander, Nano Lett. **11**, 2318 (2011).
[21] W. Zhou and T. W. Odom, Nat. Nanotechnol. **6**, 423 (2011).
[22] S. R. K. Rodriguez, A. Abass, B. Maes, O. T. A. Janssen, G. Vecchi, and J. G. Rivas, Phys. Rev. X **1**, 021019 (2011).
[23] H. Deng, G. Weihs, C. Santori, J. Bloch, and Y. Yamamoto, Science **298**, 199 (2002).
[24] J. Kasprzak, M. Richard, S. Kundermann, A. Baas, P. Jeambrun, J. M. J. Keeling, F. M. Marchetti, M. H. Szymańska, R. André, J. L. Staehli, V. Savona, P. B. Littlewood, B. Deveaud, and L. S. Dang, Nature (London) **443**, 409 (2006).
[25] R. Balili, V. Hartwell, D. Snoke, L. Pfeiffer, and K. West, Science **316**, 1007 (2007).
[26] M. A. Verschuuren, Ph.D. thesis, Utrecht University, 2010.
[27] See Supplemental Material at http://link.aps.org/supplemental/10.1103/PhysRevLett.111.166802 for details on the experiments, modeling of SLRs and plasmon-exciton polaritons, the excited molecule density in the system, and the model for the saturation of the exciton-SLR coupling.
[28] R. Houdré, R. P. Stanley, and M. Ilegems, Phys. Rev. A **53**, 2711 (1996).
[29] J. J. Hopfield, Phys. Rev. **112**, 1555 (1958).
[30] M. H. Anderson, J. R. Ensher, M. R. Matthews, C. E. Wieman, and E. A. Cornell, Science **269**, 198 (1995).
[31] K. B. Davis, M. O. Mewes, M. R. Andrews, N. J. van Druten, D. S. Durfee, D. M. Kurn, and W. Ketterle, Phys. Rev. Lett. **75**, 3969 (1995).
[32] H. Deng, H. Haug, and Y. Yamamoto, Rev. Mod. Phys. **82**, 1489 (2010).
[33] Y.-Y. Lai, Y.-P. Lan, and T.-C. Lu, Light Sci. Appl. **2**, e76 (2013).
[34] R. Houdré, J. L. Gibernon, P. Pellandini, R. P. Stanley, U. Oesterle, C. Weisbuch, J. O'Gorman, B. Roycroft, and M. Ilegems, Phys. Rev. B **52**, 7810 (1995).
[35] R. Butté, G. Delalleau, A. I. Tartakovskii, M. S. Skolnick, V. N. Astratov, J. J. Baumberg, G. Malpuech, A. Di Carlo, A. V. Kavokin, and J. S. Roberts, Phys. Rev. B **65**, 205310 (2002).
[36] P. Vasa, R. Pomraenke, G. Cirmi, E. De Re, W. Wang, S. Schwieger, D. Leipold, E. Runge, G. Cerullo, and C. Lienau, ACS Nano **4**, 7559 (2010).
[37] P. Vasa, W. Wang, R. Pomraenke, M. Lammers, M. Maiuri, C. Manzoni, G. Cerullo, and C. Lienau, Nat. Photonics **7**, 128 (2013).
[38] S. R. K. Rodriguez, S. Murai, M. A. Verschuuren, and J. G. Rivas, Phys. Rev. Lett. **109**, 166803 (2012).
[39] T. Elsaesser and W. Kaiser, Annu. Rev. Phys. Chem. **42**, 83 (1991).
[40] A. I. Tartakovskii, M. Emam-Ismail, R. M. Stevenson, M. S. Skolnick, V. N. Astratov, D. M. Whittaker, J. J. Baumberg, and J. S. Roberts, Phys. Rev. B **62**, R2283 (2000).
[41] J. Klaers, J. Schmitt, F. Vewinger, and M. Weitz, Nature (London) **468**, 545 (2010).
[42] W. Zhou, M. Dridi, J. Y. Suh, C. H. Kim, D. T. Co, M. R. Wasielewski, G. C. Schatz, and T. W. Odom, Nat. Nanotechnol. **8**, 506 (2013).